



ISSN: 0067-2904

Cu₂SnS₃ Thin Films Deposited via Automated Spray Pyrolysis System for Solar Collectors Applications

Zaid L. Hadi^{1,*}, Mohammed Sh. Essa², and Bahaa T. Chiad³

¹Ministry of Education, General Directorate of Education of Babylon, Babel, Iraq

²Department of Medical Physics, College of Applied Science, University of Fallujah, Iraq

³Department of Physics, College of Science, University of Baghdad, Baghdad, Iraq

Received: 19/12/2023

Accepted: 24/1/2025

Published: 15/2/2025

Abstract

Copper tin sulfide (CTS) thin films were deposited on glass substrates using the spray pyrolysis technique. The solution mixture was sprayed onto the glass substrate at 310°C. The CTS thin films have a monoclinic crystal structure based on XRD analysis. FTIR confirmed Cu, Sn, and S chemical bonding, whereas the Scherrer formula predicted nanoscale particle size. The AFM analysis revealed a surface roughness measurement of 42 nm. Substrates coated with CTS film showed uniformity, which revealed the coated surface shape and design. A precise measurement of the substrate temperature was made. EDX confirmed Cu-Sn-S composition. For solar collector applications, thin films deposited in CTS were treated with a blue laser source with a 405 nm wavelength.

Keywords: Cu₂SnS₃, CTS thin films, Spray pyrolysis, laser applications, solar collectors.

ترسيب اغشية Cu₂SnS₃ الرقيقة بواسطة نظام رش حراري آلي لتطبيقات المجمعات الشمسية

زيد لؤي هادي الطائي^{1*}، محمد شعلان عيسى²، بهاء طعمة جيايد³

¹وزارة التربية العراقية، المديرية العامة للتربية في بابل، بابل، العراق.

²قسم الفيزياء الطبية، كلية العلوم التطبيقية، جامعة الفلوجة، العراق.

³قسم الفيزياء، كلية العلوم، جامعة بغداد، بغداد، العراق

الخلاصة

حضرت اغشية رقيقة من كبريتيد القصدير والنحاس (CTS) على شرائح زجاجية باستخدام تقنية الرش الحراري. حيث تم رش المحلول المحضر من خليط المكونات على الشريحة الزجاجية عند درجة حرارة 310 مئوية، أثناء عملية الترسيب. ومن النتائج تبين أن اغشية CTS الرقيقة لها بنية بلورية أحادية الميل بناءً على تحليل طيف الاشعة السينية (XRD). بينما استخدمت معادلة Scherrer لحساب حجم الجسيمات بوحدة النانومتر. فيما اظهر مجهر القوة الذرية خشونة سطحية بمعدل 42 نانومتر. وأكد تحليل فورير الطيفي للأشعة تحت الحمراء الترابط الكيميائي للنحاس والقصدير والكبريت، أظهرت الشرائح المطلية بطبقة CTS تجانسا واضح

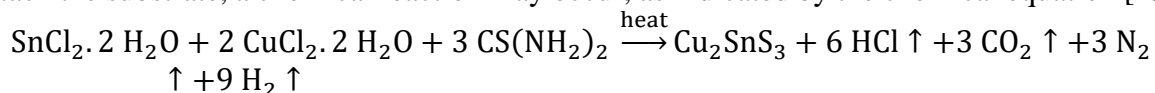
*Email: zaid.altai@outlook.com

باستخدام المجهر الإلكتروني (SEM) كما كشف عن شكل السطح للطبقة المطلوبة، حيث وجد ان التوزيع السطحي للمادة كان جيدا. كما وتم مراقبة تغيرات درجة حرارة الشريحة خلال عملية الترسيب بشكل دقيق. أكد فحص EDX على تكون مركبات Cu-Sn-S. ولغرض الدراسة من اجل التوظيف لتطبيقات المجمعات الشمسية، تم معالجة الاغشية الرقيقة المرسبة بمصدر ليزري أزرق اللون بطول موجة 405nm.

Introduction

The value attributed to renewable energy sources is continuously growing due to the rising global energy demand, the rapid exhaustion of fossil fuel supplies, and, especially, the increasing global environmental concerns [1]. Solar energy is the optimal energy source for future generations due to its practicality, cost-effectiveness, environmental friendliness, and renewable nature [2]. The spray pyrolysis technique (SPT) is a simple and efficient process that does not require vacuum. It utilizes an aqueous solution to produce a diverse array of materials in the form of thin films [3]. Moreover, SPT is classified as an economical and ecologically friendly technique for preparing thin films for use in diverse light film applications. Spray-deposited Copper Tin Sulfite (CTS) thin film research has proven unsatisfactory [4]. CTS thin films were fabricated using several techniques, including chemical bath deposition [5], sulfurization [6], solid-state reaction [7], solvothermal [8], co-evaporation [9] electrodeposition [10] in addition to the renowned technique known as spray pyrolysis [3]. Several chemical phases of copper tin sulfides are possible, such as Cu_2SnS_3 [2], $\text{Cu}_2\text{Sn}_3\text{S}_7$ [11], Cu_3SnS_4 [12], Cu_4SnS_4 [13], and $\text{Cu}_4\text{Sn}_7\text{S}_{16}$ [14]. The ternary sulfide phases (Cu_2SnS_3) are the most suitable for solar applications due to their direct band gap and high absorption coefficient. CTS absorption layers were created using a homemade Automated Spray Pyrolysis System. An aqueous solution is sprayed onto a hot plate in motion while recording the substrate temperature. Experimental results showed that thermal energy is evenly distributed on the hot plate. This project aims to produce a ternary chemical component for solar collectors.

The CTS thin films were produced in this study using an automated spraying pyrolysis method. The study utilizes a machine with a unique 3D mobility feature, enabling the hotplate platform to traverse in the x-y plane. This feature allows for the application of coatings across more significant regions than the typical size of micro slides usually utilized in laboratories. Furthermore, the machine's nozzle holder can vertically move along the z-axis, enabling precise adjustment of the distance between the nozzle and the substrate, popularly known as the nozzle-to-substrate distance (NSD). An inquiry is conducted using a fully automated system that can measure and control the temperature of the substrate concurrently. When precursor molecules attack the substrate, a chemical reaction may occur, as indicated by the chemical equation [15]:



A flow meter was used to control the movement of gas. According to this research objective, a specific laser source was utilized to enhance the surface absorption of the produced samples. The nozzle was accurately adjusted to a certain height to achieve the optimal spot size. According to Hadi and Chad [15], increasing the groove's depth improves the absorption. Laser grooving is a precise machining process that uses a focused laser beam to create narrow, accurate grooves on various materials. It is widely used in industries like electronics, automotive, and aerospace for its high precision and minimal material damage [16, 17]. For the laser grooving process, a blue laser source (405 nm) of power 1000mW was employed.

Experimental

The study employed the spray pyrolysis technique for the CTS deposition process. The deposition process used an aqueous solution containing tin chloride dihydrate ($\text{SnCl}_2 \cdot 2\text{H}_2\text{O}$),

copper chloride dihydrate ($\text{CuCl}_2 \cdot 2\text{H}_2\text{O}$), and thiourea ($\text{CS}(\text{NH}_2)_2$), with carefully selected quantities. Three different solutions were prepared at the same point of $\text{pH} = 2$. Next, the substrate, heated to a temperature of 320 ± 5 °C, was coated with a solution containing a mixture of precursors. The nozzle, with a radius of 0.35 mm, was positioned 30 cm from the substrate, and the aqueous solution was sprayed using a carrier gas pressure that had been appropriately calibrated onto the heated substrates at a rate of about 0.1 mL/sec. Chemical interactions occurred between the substrate and the source ingredients in the aqueous phase. Several samples were deposited during the present work; the optimum one was selected according to the startup concentration.

X-ray diffractometer (D2 PHASER), which used Cu-K radiation of (1.54056 Å) wavelength, was used to examine the structure of the thin films. Debye-Scherrer's formula, depicted in Equation 1, was applied to XRD patterns to estimate the crystallite size [15]:

$$D_{hkl} = \frac{K \lambda}{\beta \cos(\theta_{hkl})} \quad (1)$$

The thickness of CST thin films was measured using an optical interferometer using a green laser with a wavelength of 532nm. Having a clear understanding of this method depends on the light beam reflecting the surface of the substrate and the thin film. Employing Equation 2, thickness was calculated:

$$t = \frac{\lambda}{2} \times \frac{\Delta x}{x} \quad (2)$$

where Δx is the interference fringe displacement, and x is the distance between two neighboring fringes. This is known as Fizeau Fringes interferometric method.

FTIR spectrophotometer (Shimadzu IR Prestige-21, a Japanese instrument) was used to verify the FTIR spectrum. UV-visible spectroscopy (K-MAC SV2100) was used to conduct UV-visible spectroscopy at ambient temperature. A Scanning Probe Microscope (SPM) (model AA3000) was used to examine the surface structure of the formed layer. A temperature data logger (BTM-2048SD) was used to examine temperature variance and thermal absorbing enhancement. To investigate the thermal absorbing process, seven different samples were used.

Results

XRD analysis revealed the crystal structure of CTS thin films. Figure 1 shows the diffraction pattern of CTS thin film. It was observed that the CTS sample exhibits a polycrystalline structure with a monoclinic phase. In addition to the peaks of 2θ of 28.45° , 32.68° , 47.31° , and 56.38° , there were also peaks related to the scattered X-ray. The highest reflection intensity was found at the first peak. The plotted patterns were explained in COD card numbers (96-152-6188) reported by Onoda et al. [18].

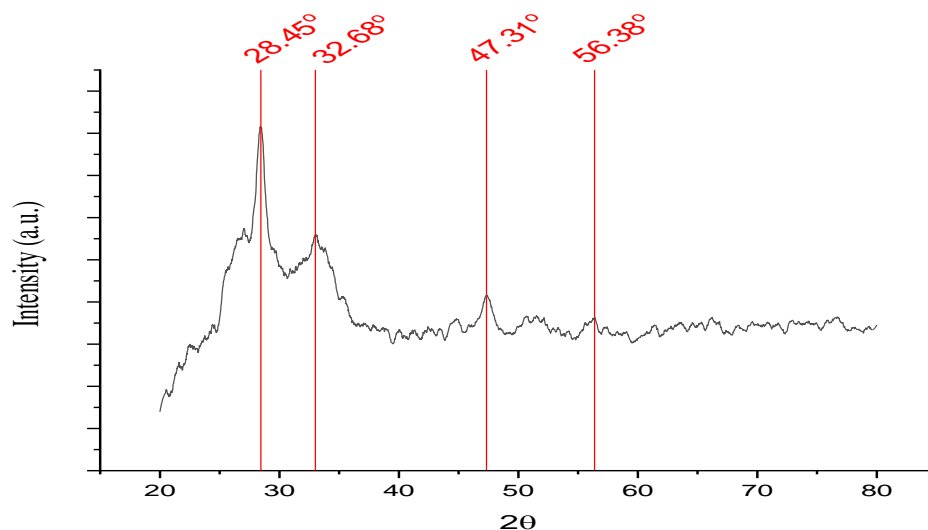


Figure Error! No text of specified style in document.1: XRD pattern of CTS thin film as deposited.

According to Debye-Scherrer's formula, there was a high degree of accuracy of about 99% in the agreement between the measured values of diffraction angles and d-spacing and the typical values obtained from the XRD analysis [19]. The observed size of the crystallite was around 90 nm. The average thickness of the ideal sample was determined to be about 185 nanometers.

Figure 2 illustrates the FTIR spectrum of the Cu_2SnS_3 thin film. The narrow band observed at 450 cm^{-1} is attributed to the Cu-O vibrational link in copper oxides, namely Cu_2O and CuO . The vibrational frequencies within the specified range were attributed to the Cu-S, Sn-S, Sn (IV)-O, and Sn(II)-O bonds. This result was also reported by Helan et al., [20]. At the spectral region of $2300\text{--}2000\text{ cm}^{-1}$, there are faint bands that have been identified in previous studies as potentially corresponding to the $\text{C}\equiv\text{S}$ and nitrile bond $\text{C}\equiv\text{N}$ [21]. Furthermore, there are additional vibrations of amide N-H, alcohol O-H, and alkyne CH bonds, which are distinctly observed within the area of $3500\text{--}3350\text{ cm}^{-1}$ [22].

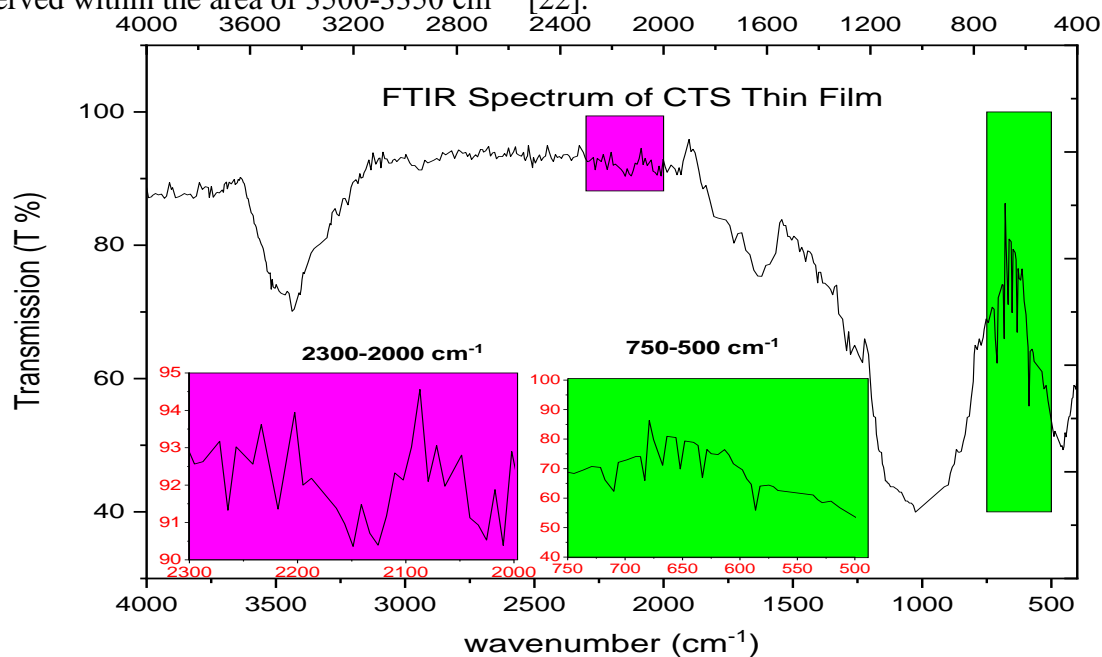


Figure 2: FTIR spectrum of CTS thin film.

Figure 3 displays a UV–Vis spectrum of the CTS thin film. As per the source [23], Absorption and transmission are depicted in an illustration. As a result of the grooving process, the range will be determined. Calibration was performed by dividing the absorbance measurements by the column's most significant value. Moreover, the laser grooving increased the surface area of the thin layer, enhancing CTS absorption.

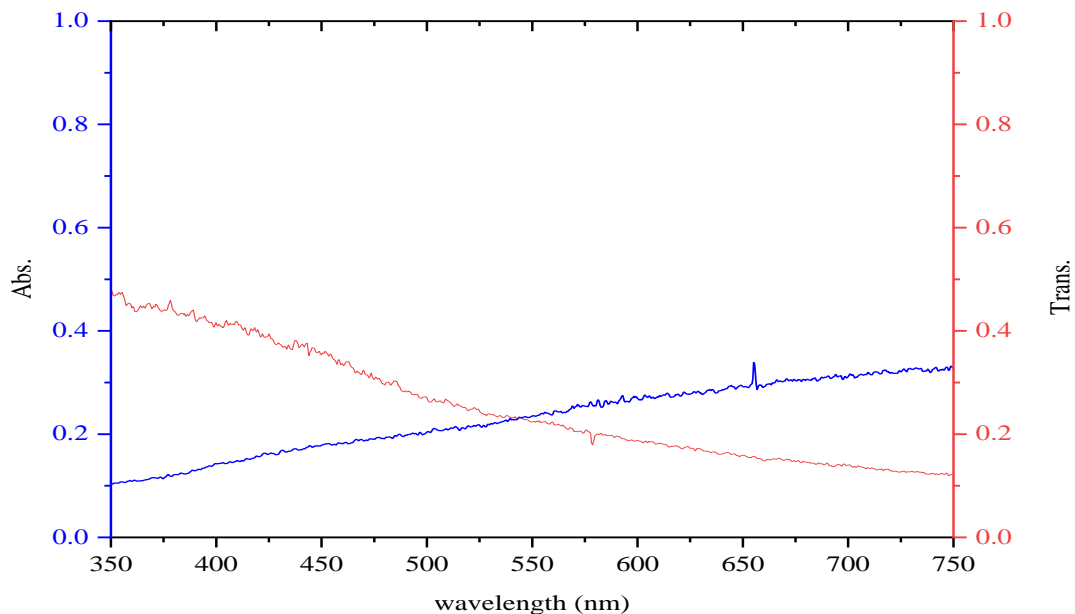


Figure 3: The UV-Vis spectrum of CTS thin film.

An atomic force microscope was used to analyze CTS thin films. The 3D image and grain size distributions of the deposited CTS thin film are displayed in Figure 4. Based on AFM micrographs, the surface exhibited a consistent distribution of grains throughout $4 \mu\text{m}^2$ region. The average particle size measured was 120 nanometers, whereas the surface roughness was 42 nanometers. The light absorption is directly proportional to the roughness of the surface as the surface area expands.

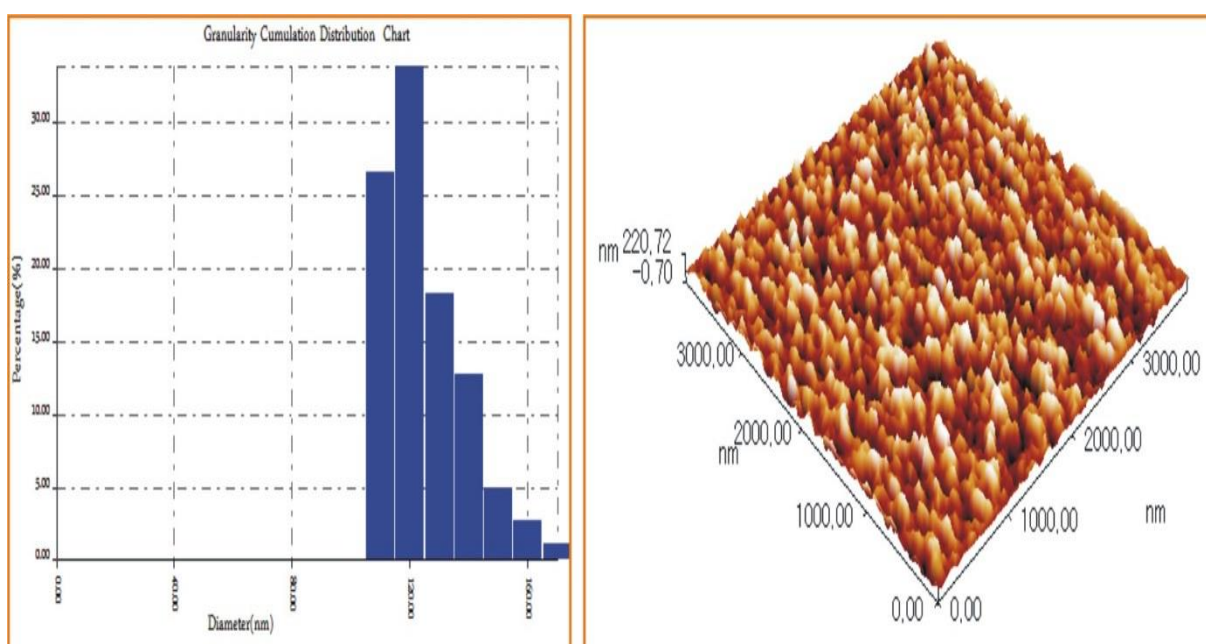


Figure 4: AFM of CTS thin film.

Figure 5 displays scanning electron micrographs (SEM) of CTS thin films taken at various magnifications, showing how these films are dense, compact, and uniform when produced under optimal conditions as opposed to other films made in the current work under different concentrations.

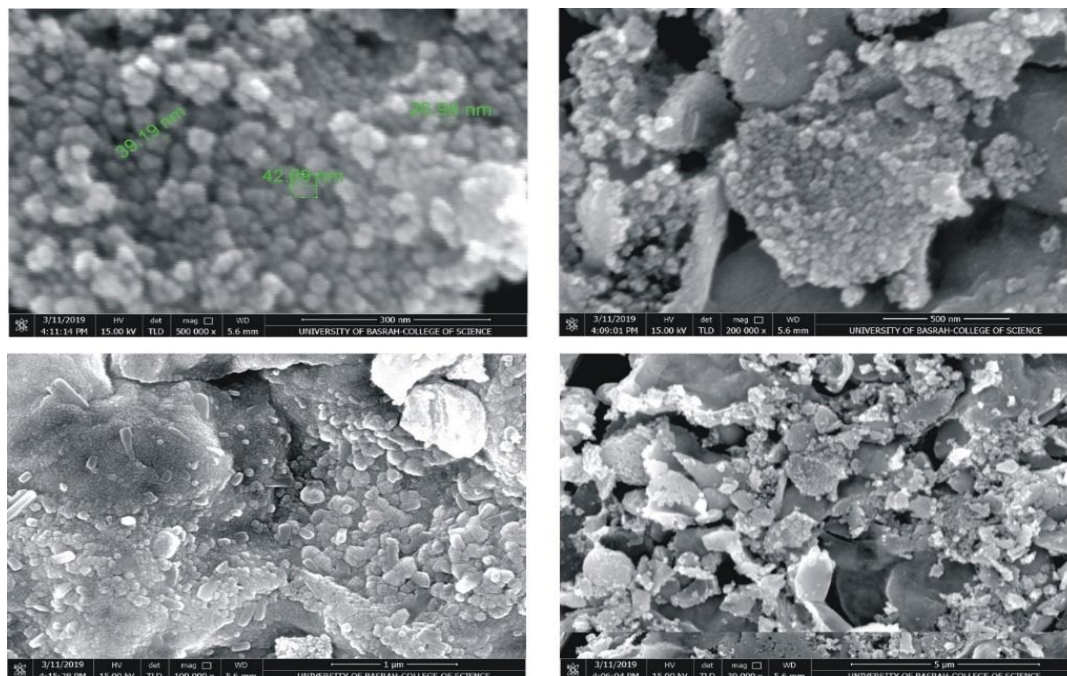


Figure 5: SEM imaging of CTS thin film at different magnification scales.

The produced samples' absorbance efficiency was measured using a calibrated data recording equipment. The absorbance efficiency was assessed by analyzing the data. The temperature obtained for the chosen samples over time is depicted in Figure 6, which demonstrates that the grooved layer absorbs less light than the as-deposited layer. Eight channels were active for this experiment, and the data logger recorded data every 10 seconds across these channels, as shown in Table 1. Every sample has the same measurements as glass slides used in laboratories.

Table 1: Channel distribution of data logger recordation.

Channel number	Sample
Ch1	Un-grooved as-deposit CTS Thin Film
Ch2	Grooved CTS Thin Film
Ch3	Low Thickness Un-grooved CTS Thin Film
Ch4	NiO Thin Film
Ch5	Copper Alloy
Ch6	Tin-Zinc Alloy
Ch7	Alumina alloy
Ch8	Ambient Air

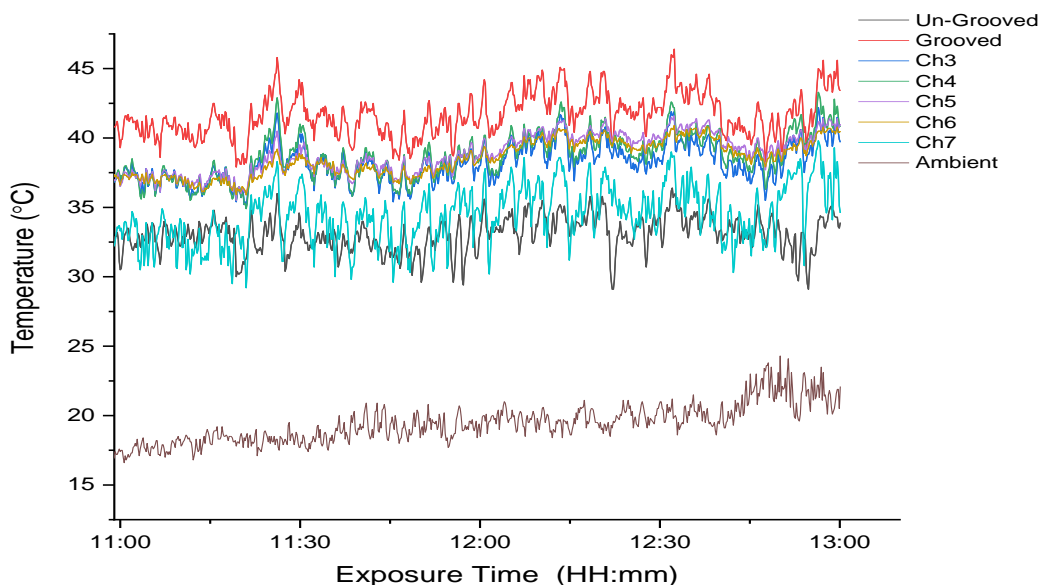


Figure 6: Temperature record of the stack samples using a data logger device.

According to Figure 7, the grooved surface shows a higher average temperature of around 8.30°C than that of the un-grooved sample, which shows a comparable rise of 25%. Furthermore, for both grooved and un-grooved CTS samples, the mean temperature curve values were 41.4°C and 33.1°C , respectively, whereas ambient temperatures were 18.6°C , respectively. Heat transfer through CTS thin films was done via a data logger device, In order to carry out the temperature that the CTS thin film transferred. It is worth mentioning that the laser grooving process increases the surface area of the prepared samples. Therefore, when the area increases, the energy absorbed where increases too.

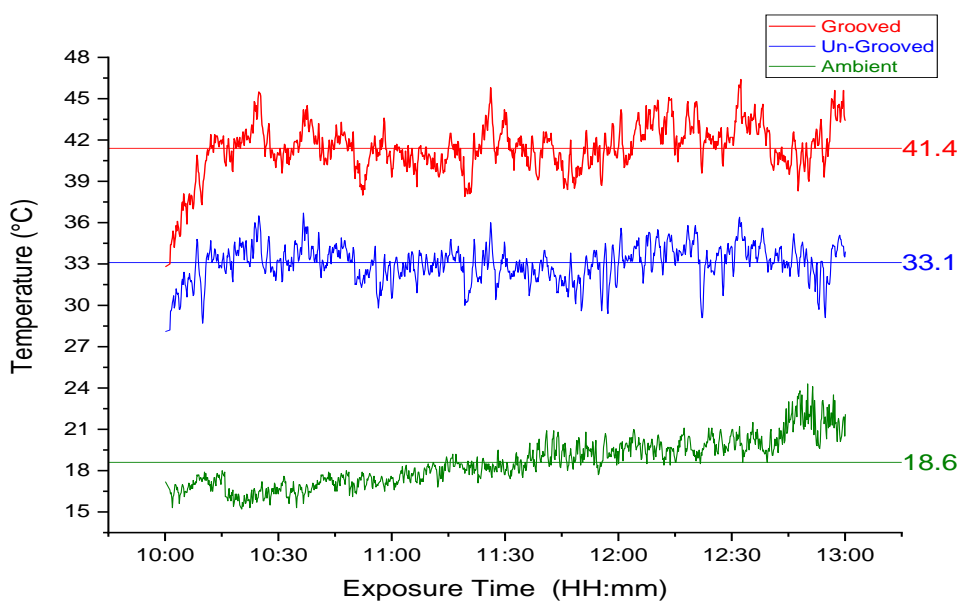


Figure 7: Enhancement of absorbing temperature of grooved and un-grooved layers.

Conclusion

Spray pyrolysis, under ideal conditions, successfully deposited CTS thin films onto glass substrates. XRD examination revealed that the films have a monoclinic structure. The FTIR

examination of nanoscale grains showed the presence of both Cu-S and Sn-S bonds. To increase surface area and, consequently, absorption, laser beams made microscale grooves in the deposited layer. A suitable spot size laser source was used to achieve precise groove width. When it comes to heat absorption efficiency, grooved surfaces outperform non-grooved surfaces by about 25%. Depending on the application, many laser sources can be used for laser-grooving systems.

References

- [1] N. Akcay, V. F. Gremenok, Y. Ozen, K. P. Buskis, E. P. Zaretskaya, and S. Ozcelik, "Investigation on photovoltaic performance of Cu₂SnS₃ thin film solar cells fabricated by RF-sputtered In₂S₃ buffer layer," *J Alloys Compd*, vol. 949, p. 169874, 2023,
- [2] X. Liu et al., "Fabrication of Cu₂SnS₃ thin film solar cells via a sol-gel technique in air," *Physica B Condens Matter*, vol. 627, p. 413613, 2022,
- [3] Z. L. Hadi and B. T. Chiad, "Study of mixing different volume ratios for preparing Cu₂SnS₃ thin films using computerized spray pyrolysis system," *Iraqi Journal of Science*, vol. 60, no. Special Issue, pp. 22–27, 2019,
- [4] A. B. Workie, H. S. Ningsih, and S.-J. Shih, "An comprehensive review on the spray pyrolysis technique: Historical context, operational factors, classifications, and product applications," *J Anal Appl Pyrolysis*, vol. 170, p. 105915, 2023,
- [5] J. Rakspun, N. Kantip, V. Vailikhit, S. Choopun, and A. Tubtimtae, "Multi-phase structures of boron-doped copper tin sulfide nanoparticles synthesized by chemical bath deposition for optoelectronic devices," *Journal of Physics and Chemistry of Solids*, vol. 115, pp. 103–112, 2018,
- [6] M. R. Pallavolu, V. R. Minnam Reddy, B. Pejjai, D. Jeong, and C. Park, "Effect of sulfurization temperature on the phase purity of Cu₂SnS₃ thin films deposited via high vacuum sulfurization," *Appl Surf Sci*, vol. 462, pp. 641–648, 2018,
- [7] D. Tiwari, T. K. Chaudhuri, T. Shripathi, and U. Deshpande, "Synthesis of earth-abundant Cu₂SnS₃ powder using solid state reaction," *Journal of Physics and Chemistry of Solids*, vol. 75, no. 3, pp. 410–415, 2014,
- [8] Y. Tan, Z. Lin, W. Ren, W. Long, Y. Wang, and X. Ouyang, "Facile solvothermal synthesis of Cu₂SnS₃ architectures and their visible-light-driven photocatalytic properties," *Mater Lett*, vol. 89, pp. 240–242, 2012,
- [9] V. Robles, J. F. Trigo, C. Guillén, and J. Herrero, "Copper tin sulfide (CTS) absorber thin films obtained by co-evaporation: Influence of the ratio Cu/Sn," *J Alloys Compd*, vol. 642, pp. 40–44, 2015,
- [10] N. R. Mathews, J. Tamy Benítez, F. Paraguay-Delgado, M. Pal, and L. Huerta, "Formation of Cu₂SnS₃ thin film by the heat treatment of electrodeposited SnS–Cu layers," *Journal of Materials Science: Materials in Electronics*, vol. 24, no. 10, pp. 4060–4067, 2013,
- [11] S. Fiechter, M. Martinez, G. Schmidt, W. Henrion, and Y. Tomm, "Phase relations and optical properties of semiconducting ternary sulfides in the system Cu–Sn–S," *Journal of Physics and Chemistry of Solids*, vol. 64, no. 9–10, pp. 1859–1862, 2003,
- [12] M. Dong, L. Wei, and Y. Zhu, "Controllability study of copper-tin-sulphide (Cu₃SnS₄) material based on the ratio adjustment of Cu to Sn elements," *Micro Nano Lett*, vol. 18, no. 9–12, 2023,
- [13] D. Avellaneda, A. Paul, S. Shaji, and B. Krishnan, "Synthesis of Cu₂SnS₃, Cu₃SnS₄, and Cu₄SnS₄ thin films by sulfurization of SnS–Cu layers at a selected temperature and /or Cu layers thickness," *J Solid State Chem*, vol. 306, p. 122711, 2022,

- [14] J. P. F. Jemetio, P. Zhou, and H. Kleinke, "Crystal structure, electronic structure and thermoelectric properties of Cu₄Sn₇S₁₆," *J Alloys Compd*, vol. 417, no. 1–2, pp. 55–59, 2006,
- [15] Z. L. Hadi and B. T. Chiad, "Investigation of Laser Grooving Process on Copper Tin Sulfite Thin Films," *J Phys Conf Ser*, vol. 1178, no. 1, p. 012033, 2019,
- [16] Y. Chen, Y. Shao, and X. Xiao, "A new method for predicting the morphology and surface roughness of micro grooves in aluminum alloy ablated by pulsed laser," *J Manuf Process*, vol. 96, pp. 193–203, 2023,
- [17] C. Wu, T. Zhang, W. Guo, X. Meng, Z. Ding, and S. Y. Liang, "Laser-assisted grinding of silicon nitride ceramics: Micro-groove preparation and removal mechanism," *Ceram Int*, vol. 48, no. 21, pp. 32366–32379, 2022,
- [18] M. Onoda, X. A. Chen, A. Sato, and H. Wada, "Crystal structure and twinning of monoclinic Cu₂SnS₃," *Mater Res Bull*, vol. 35, no. 9, pp. 1563–1570, 2000,
- [19] P. Debye and P. Scherrer, "Interference of irregularly oriented particles in x-rays," *Phys. Ziet*, vol. 17, pp. 277–283, 1916,
- [20] J. Helan *et al.*, "Ethylenediamine Processed Cu₂SnS₃ Nano Particles via Mild Solution Route.," *Journal of New Materials for Electrochemical Systems*, vol. 19, no. 1, pp. 1–5, 2016.
- [21] P. Zhao and S. Cheng, "Influence of sulfurization temperature on photoelectric properties Cu₂SnS₃ thin films deposited by magnetron sputtering," *Advances in Materials Science and Engineering*, vol. 2013, pp. 1–4, 2013,
- [22] S. Biniak, G. Szymański, J. Siedlewski, and A. Świątkowski, "The characterization of activated carbons with oxygen and nitrogen surface groups," *Carbon NY*, vol. 35, no. 12, pp. 1799–1810, 1997,
- [23] X. Liang *et al.*, "Preparation and Characterization of Flower-like Cu₂SnS₃ Nanostructures by Solvothermal Route," *J Mater Sci Technol*, vol. 29, no. 3, pp. 231–236, 2013,